Local density of unoccupied states in ion-beam-mixed Pd-Ag alloys

K. H. Chae, S. M. Jung, Y. S. Lee, and C. N. Whang
Department of Physics, Yonsei University, Seoul 120-749, Korea

Y. Jeon
Department of Physics, Jeonju University, Jeonju 560-759, Korea

M. Croft and D. Sills
Department of Physics and Astronomy, Rutgers University, Piscataway, New Jersey 08855-0849

P. H. Ansari and K. Mack
Department of Physics, Seton Hall University, South Orange, New Jersey 07079
(Received 28 August 1995; revised manuscript received 10 November 1995)

X-ray absorption spectroscopy (XAS) measurements have been used to probe the electronic structure of ion-beam-mixed (IBM) Pd-Ag thin films with bulk alloys being studied for comparison. Pd L_3 and Ag L_3 absorption edges for pure Pd, Ag, and $Pd_{1-x}Ag_x$ alloys are discussed. Structural information from both x-ray diffraction and the XAS fine structure oscillations are discussed. The observed decrease of the white-line feature strength, at the Pd L_3 edge, indicates that the local density of unoccupied Pd $4d$ states declines upon alloying with Ag in a manner similar to that observed in previous bulk studies. However, while the Pd d-hole count decreases monotonically for bulk alloys, in the IBM alloys it saturates at higher levels in the Ag-rich materials. This disparity is interpreted on the basis of a modified charge transfer due to structural differences in the IBM alloys. The Ag L_3 near-edge region is largely unchanged in these alloys, indicating that the charge transferred away from the Ag site is dominantly of *non-d* type. Our experimental results are discussed in the context of recent electronic structure calculations and of previous work on this alloy system.

I. INTRODUCTION

Ion-beam mixing has been of great interest as a method to produce new metastable alloys and structures which do not exist in the equilibrium state.[1] Thin films prepared by ion-beam mixing or implantation have been used to prepare materials with new structural (e.g., amorphous and quasicrystalline) or physical (e.g., metallic versus insulating) properties.[2] In the ion-beam mixing technique, the alloy or compound is formed due to the atomic interaction between different species during the mixing process. However, the interrelation between chemical reaction and physical atomic collisions in such a situation is not completely understood due to the complexity of the mixing phenomenon.

Insight into the electronic structure is a prerequisite to fundamental understanding of the physical and chemical properties of a solid. Recently some application of the popular photoemission based electron spectroscopies have been made to probe ion-beam-mixed (IBM) materials.[3] However, the requisite surface preparation methods complicate such electron spectroscopies with possible alteration of metastable phases or stoichiometries. As a consequence research into the electronic structure of ion-beam-mixed materials, especially the nonequilibrium ones, has not been extensive.

X-ray absorption spectroscopy (XAS) provides an attractive route to probe both the structure and electronic states of ion-beam modified materials.[4,5] The photon penetration depth allows study of the interior of the films without the necessity of specialized surface preparation.[6,7] Structural information can be extracted from the extended x-ray absorption fine structure (EXAFS) oscillations and upon occasion (as we will show here) from the fine structure oscillations closer to the edge.[6,8,9] XAS studies of the near-edge region (within 50 eV of the edge) can be used to study the electronic states just above the Fermi level (E_F) on an atom-specific and orbital angular momentum-specific basis.[10,11] Moreover, such XAS studies can usually be extended (as we have done here) to each of the atomic sites in the material. In this paper we employ XAS to study ion-beam-mixed alloys and for comparison selected bulk alloys, in the Pd-Ag system. The electronic structure information gained from these measurements will be correlated with structural results. In addition to addressing the charge transfer issues in this alloy system, this work is intended to establish the techniques needed for wider studies of charge transfer in IBM materials some of which are metastable.

Near-edge L_3 XAS has been used extensively in recent years to study both the d-hole count and the distribution of d states above E_F in noble metal and transition-metal compounds.[5,12–21] These studies focus on the so-called ''white line'' (WL) features at the transition metal $L_{2,3}$ edges. These WL features are caused by transitions from the core $2p$ level into empty d states above E_F in the solid.[10,11] From such WL studies Bzowski and Sham, for example, inferred an increase in the number of *sp-like* conduction electrons and a decrease in the number of d electrons at the Pd sites occurred upon alloying with Ti.[18] They also found a similar charge redistribution in the Au-Ti system.[19,22] In our previous study of metastable ion-beam-mixed Au-Si films, we found that the Au $5d$-hole count increased with the concentration

of Si due to metastable compound formation.[5] For these metastable Au-Si materials, it was proposed that the Au sites gained sp-type electrons (in accordance with electronegativity) and lost d-electrons to maintain charge neutrality.

Regarding the Pd-Ag system discussed here, Cordts *et al.*[14] performed a tour de force, presynchrotron, low energy, XAS study of the Ag and Pd L_3 edges in flash evaporated thin films in the 0–60 % Ag range. Although this study necessarily had limited resolution and relied on a finite thickness correction procedure to extract the spectra, it yielded several important observations. The observed Pd L_3 WL feature diminution with increasing Ag concentration was associated with Pd d-band filling. The robust remnant Pd L_3 feature, above 40% Ag substitution, was noted to disagree with the filled Pd d-band results in the CPA calculation of Stocks *et al.*[23] Finally, upon careful comparison of the Pd L_3 WL results to Eggs *et al.*'s[24] isochromat spectroscopy results, the two were concluded to be consistent.

In this paper we report high resolution, synchrotron based Ag/Pd L_3-edge XAS measurements on ion-beam-mixed and selected bulk $Pd_{1-x}Ag_x$ alloys. Although our equilibrium $Pd_{1-x}Ag_x$ alloy spectral results have higher energy resolution and do not require thickness corrections, our bulk results basically confirm the observation of Cordts *et al.*[14] regarding the Pd L_3 WL feature variation. The central focus of our study will be the more extensive ion-beam-mixed material studies. Our structural and Pd/Ag sphere charge transfer results will be discussed in the context of recent electronic structure calculations and of the atomic volume dependence of the charge transfer in the macroscopic atom model.

II. EXPERIMENT

The starting multilayers consisted of three pairs of Pd and Ag layers, with the thicknesses of each layer being varied to set the alloy composition. These multilayers were deposited on a Si substrate by sequential electron-beam evaporation at a base pressure of less than 2×10^{-7} torr and a deposition pressure of 8×10^{-7} torr. The total thickness of the multilayer film, roughly 500 Å, was chosen to match with the projected range of the 80 keV Ar^+ mixing ions. The ion-beam mixing dose was 1.5×10^{16} Ar^+/cm^2 at room temperature with a current density limited to 1.5 $\mu A/cm^2$ to avoid thermal effects. The concentration of ion-beam-mixed thin film was measured by Auger electron spectroscopy (AES) depth profiling, and the film homogeneity was verified. The bulk Pd-Ag alloys were prepared by standard argon arc-furnace techniques.

The Pd and Ag L_3 edge XAS measurements were performed at the National Synchrotron Light Source (NSLS) at Brookhaven National Laboratory on beamline X-19A. The x-ray energy was varied using a Si(111) double-crystal monochromator which was detuned by 50% to minimize higher order harmonic beam content. The X-19A beamline optics are maintained at ultrahigh vacuum up to the 10-mil thick beryllium exit window. This configuration gives X-19A a high beam intensity all the way down to 2.15 keV, which makes it well suited for measuring $L_{2,3}$ absorption spectra on $4d$-row transition-metal compounds.

The spectra were collected in the total electron yield (EY) mode in which the photo-induced secondary electron current is used to measure the absorption coefficient.[25] Studies have shown that the secondary electron escape depth is in the 1000 Å range.[7,26] Since the secondary electron escape depth exceeds the film thickness and since the ion-beam mixing parameters were designed to produce homogeneous films, this method provides a good sampling of these IBM alloys.

In general the EY method is almost required for $4d$-row $L_{2,3}$-WL studies and has been used extensively as a standard method in low energy XAS studies.[20,27] There are several reasons for the electron yield method being the method of choice for $4d$-row studies: the short x-ray absorption length in this 2 – 3.4-keV range; the substantial degradation of the WL feature due to thickness[28] or self-absorption[29] effects for samples not in the thin absorber limit; the difficulty in preparing and characterizing thin film compounds; and finally the fact that the e^--escape depth insures the thin sample limit even for bulk materials. In extensive studies of $5d$-row compounds the authors have confirmed in some detail the correlation of the EY mode results with traditional transmission mode absorption coefficient measurements.[17]

The spectra in this paper have been background subtracted and normalized as follows. A linear fit of the preedge absorption coefficient energy variation for photons of energy less than the absorption threshold was subtracted from each raw spectrum. The resulting curves were normalized by multiplying a factor which made the continuum step equal to unity at higher energy.

The structure of these ion-beam-mixed films was studied by grazing-angle x-ray diffraction (GXRD) using a SINTAC diffractometer. The intense 111-film reflection was used to determine the lattice parameter with the 111-Si substrate reflection being used as an internal standard. It should be noted that a series of diffraction measurements were carried out at differing fixed-film-orientation-angles, as well as in the standard theta-2-theta mode. The effective cubic cell parameters in all of the measurements were essentially the same for a given alloy. This indicates that the lattice parameter variations, discussed later, are due to alloy volume effects and are so discussed.

III. RESULTS AND DISCUSSION

A. Structure

The average lattice constant, a, determined from our GXRD measurements for the IBM alloys is plotted in Fig. 1 versus the Ag concentration. The monotonic response of the lattice parameter to alloy composition indicates that atomic scale mixing was achieved over the entire alloy range. It should be noted that the average lattice constant of IBM alloys deviates somewhat from those of the bulk alloys, where the lattice spacings of the bulk solid solution were obtained from Ref. 30. In the Ag rich portion of the alloy series the compression of the IBM materials correlates well with previous results in which a compressive stress in ion-irradiated materials is frequently observed.[31]

In Fig. 2 we present selected result of Ag L_3 edge measurements for IBM alloys in the 51 – 100 % Ag concentration range. All of the spectra are quantitatively similar to that of elemental Ag, as will be discussed later in terms of Pd/Ag charge-transfer effects. The small oscillations in the absorption coefficient, at energies above the steeply rising edge

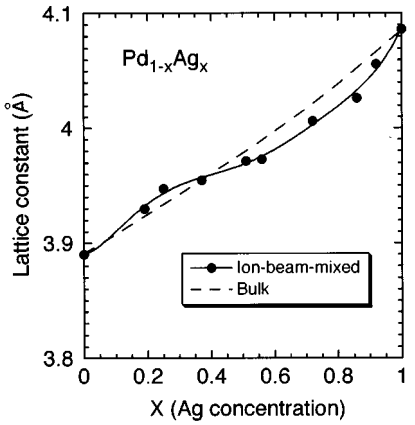

FIG. 1. Lattice constant versus Ag concentration estimated from the results of GXRD for ion-beam-mixed Pd-Ag films. The dashed line is the bulk lattice spacings results of Coles *et al.* (Ref. 30).

onset, are referred to as the fine structure (FS) features.[6,8,9] The FS features are caused by the interference of photoelectron backscattering from the near-neighbor atoms. The details of this process can involve both single and multiple scattering and can be quite complicated.[6,8,9] However, it is well established both empirically and theoretically that the feature locations and/or frequencies of the FS oscillations are sensitive to the near-neighbor distances around the absorbing atom.[9] It can be seen in Fig. 2 that the individual FS peaks shift toward higher energy with increasing Pd concentration. In the standard single scattering EXAFS analysis this would indicate that the near-neighbor distances around the Ag are decreasing with increasing Pd concentration.[6,8,9] This is not unexpected since the unit cell parameters of Ag and Pd are 4.0862 Å and 3.8898 Å, respectively, and was commented upon by Cordts *et al.*[14]

It would be useful to quantitatively correlate the FS feature shifts with the lattice parameter changes. Such a verification is complicated by the limited energy range above the Ag L_3 edge (which will not support traditional EXAFS analysis) and by the multiple shell contributions to the fcc structure FS oscillation in this energy range.

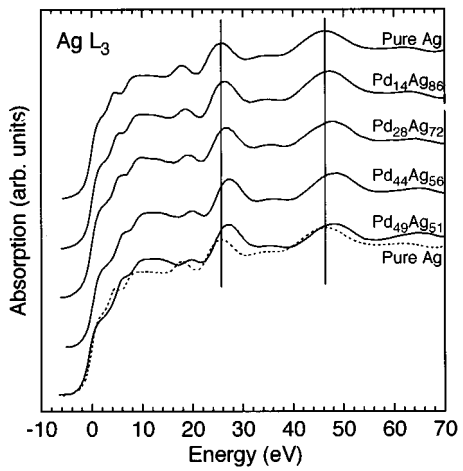

FIG. 2. Ag L_3 absorption near-edge spectra in a series of ion-beam-mixed Pd-Ag thin films. All data are normalized to unity step height energy well above the edge.

In Fig. 3(a) we present the results of a multiple scattering calculation for fcc-Ag (including 10 atomic shells with $a=4.086$ Å) using the University of Washington FEFF6 computer code.[32,33] Comparison of the calculated FS peak positions to those of our experimental spectra shows a very good correlation in the energy range above 20 eV [see Fig. 3(a)]. Electronic effects are presumably responsible for the model and/or experimental disparity close to the edge. No Debye-Waller damping was included in the calculated spectrum hence the greater FS amplitude in the calculation. The FS shifts to be expected upon lattice compression are illustrated in Fig. 3(b) where $a=4.068$ Å and $a=3.921$ Å multiple scattering calculations for fcc-Ag are compared. The distinctive lattice compression induced FS feature energy shifts are clear.

Within single scattering EXAFS theory[9] the oscillatory portion of the FS involves the interatomic distance (r) through the variable kr.[6,8,9] The k-dependent backscattering amplitude, Debye Waller factor, and electron-energy-loss factors enter as longer k-space modulation factors. Here the photoelectron wave number (k) is related to the photon energy (E) by $k=[2m(E-E_0)/\hbar^2]^{1/2}$ and E_0 is the continuum onset energy. The lattice parameter is an appropriate distance scale variable for the single and multiple scattering path lengths in a given structure. Thus we will assume that the FS oscillations should scale with the variable ka. To illustrate the appropriateness of this notion we show in Fig. 3(c) the collapse of the calculated curves [plotted in Fig. 3(b)] when plotted versus the variable ka, with the lattice parameter (a) assuming the appropriate values for the respective simulations.

In Fig. 3(d) we show the results of applying this method to the $Pd_{1-x}Ag_x$ $x=1.0$, 0.9, and 0.51 ion-beam-mixed alloy spectra. The scale variable a^* for the two alloy system has been adjusted to collapse the plots onto the pure Ag (i.e., $x=1.0$) spectrum. The a^* values thus determined are local estimates of the fcc lattice constant as seen by the absorbing Ag atom. This local view should be dominated by the nearest-neighbor distances. The fact that the atomic backscattering factors of Pd $(Z=46)$ and Ag $(Z=47)$ are so close makes it reasonable to neglect the changing alloy composition in this approximation. It should be noted that the data collapse is rather good (despite somewhat varying backgrounds). Within this method the error bars on the a^* values are roughly ± 0.02 Å which places them in quantitative agreement with the x-ray diffraction results.

The FS changes above the Pd L_3 edge also reflected the lattice dilation between Pd and Ag, thereby reconfirming the atomic scale mixing. It should be noted that, in the Ag rich alloys, some evidence for an effective Pd site dilation above the diffraction results was noted. The data quality were not, however, of sufficient quality to definitively verify this trend. Careful K-edge EXAFS and x-ray diffraction measurements on bulk materials would be useful to examine the local volume effects in this alloy system.

B. Electronic states

In Fig. 4 we show the Pd L_3 x-ray absorption near-edge spectra of as-deposited and ion-beam-mixed $Pd_{28}Ag_{72}$ multilayered films. The Pd L_3 absorption-edge spectra of pure Pd

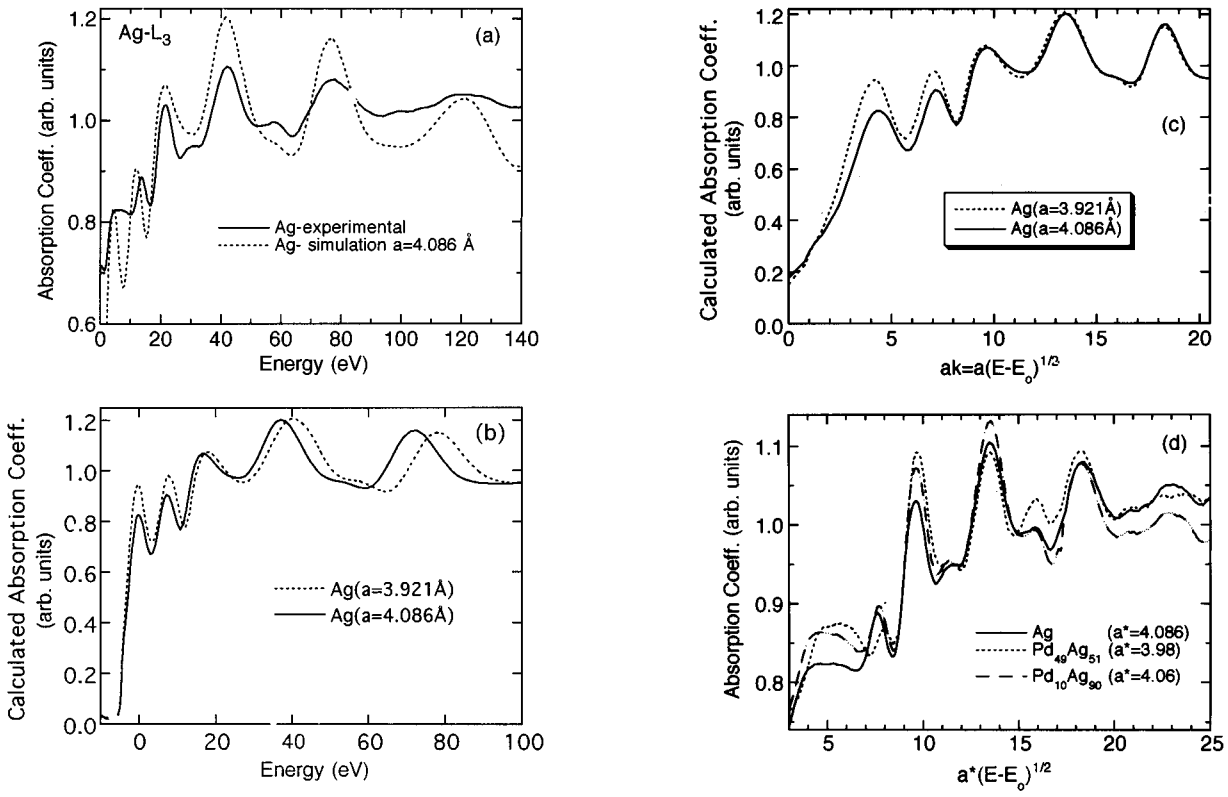

FIG. 3. (a) A superposition of the FEFF6 multiple scattering calculation of the fine structure (FS) of the elemental Ag L_3 spectrum with the experimental results. Note that the principle FS features, above 15 eV, are well aligned despite some background differences. (b) An illustration of the energy shift of the FS features induced by a lattice compression using the FEFF6 multiple scattering calculations for fcc-Ag L_3 edge with two lattice parameters. (c) An illustration of the collapse of the calculated absorption coefficients curves (from the previous figure) when the absorption coefficient is plotted versus ak, where k is the photoelectron wave number and a is the fcc lattice parameter. (d) A plot of the experimental Ag L_3 FS region for elemental Ag and two IBM alloys, $Pd_{49}Ag_{51}$ and $Pd_{10}Ag_{90}$. The scale parameter a^* has been chosen to collapse the data and represent a local estimate of the lattice contraction with increasing Pd content.

and the bulk $Pd_{25}Ag_{75}$ alloy are also shown for comparison. In addition to the FS type features discussed previously, the intense WL feature peak occurring between -3 and $+4$ eV can be clearly seen. As alluded to above, this Pd L_3 WL feature is associated with $2p_{3/2}$-core to $4d_{5/2,3/2}$-band transitions. Within the single-particle Fermi Golden Rule approximation the strength of the Pd L_3 WL should be proportional to the number of Pd $4d$ orbital holes.[34]

We note in Fig. 4 that the WL features of the as-deposited film and pure-Pd are identical as expected from the large thickness of the multilayers, that the WL features of the ion-beam-mixed alloy film and the bulk alloy are distinctly reduced in strength relative to that of pure Pd, and that the IBM WL features are broader than those of the bulk materials. In our analysis below we will see that the quantitative WL area falls off with Ag substitution less quickly for the IBM alloys, as a result mainly of this last WL broadening effect. These effects will be discussed in terms of the charge transfer between the Pd and Ag atoms in the ion-beam-mixed and bulk materials.

Figure 5 shows the Pd L_3 absorption edge spectra for various ion-beam-mixed Pd-Ag films. As in Fig. 4, the strength of the Pd WL feature can be seen to be reduced dramatically with increasing Ag concentration. The reduction of the WL strength indicates that the unoccupied density of d states projected onto the Pd atomic sphere is reduced upon alloy formation with Ag. This trend is consistent with the picture of charge transfer from the atomic partner with higher total electron density to the one with the lower.[35] It is clear that the charge transfer to the Pd site contributes to the filling of the empty Pd d states as has been suggested in bulk studies.[14]

Before turning to a quantitative discussion of the Pd L_3 WL-feature estimates of the Pd d-band filling, we will return briefly to our Ag L_3 edge results shown in Fig. 1. We note a number of points regarding the Ag L_3 near-edge spectra of these materials. For elemental Ag the absence of a white line feature reflects the fact that there are essentially no $4d$ holes in elemental Ag.[21] The spectra for the ion-beam-mixed Pd-Ag films are all similar to that of elemental Ag with respect to the absence of a WL feature. This would seem to imply that the d-hole count of Ag is not changed by alloy formation with Pd. Thus, we suggest that Ag non-d charge is transferred to the Pd sites upon alloying, thereby inducing the reduction of the white line feature of the Pd L_3 spectra. This result is consistent with the result of recent theoretical calculation of Lu *et al.*[35] using the ''special-quasirandom-structure'' (SQS) concept in which Ag loses mainly sp charge while Pd gains d charge in forming the PdAg alloy.

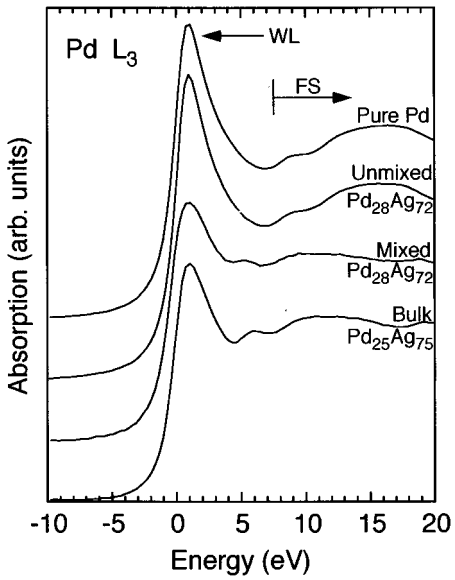

FIG. 4. The Pd L_3 near-edge spectra for bulk-elemental Pd, the as-deposited multilayered and IBM $Pd_{28}Ag_{72}$ material, and the bulk Pd_{25} Ag_{75} alloy.

In Fig. 6 we show the Pd and Ag site projected *d*-symmetry density of states for PdAg, along with those of the elements, from the calculations of Lu *et al.*[35] One point to note, in the DOS calculation, is the tailing of the Ag *d* DOS toward the Fermi energy in the alloy, through hybridization with the Pd *d* states. Thus some weak Ag *d* character at E_F is consistent with these calculations. In Fig. 7 we show an expanded view of the edge onset region of the Ag L_3 edges of elemental Ag and the $Pd_{49}Ag_{51}$ IBM alloy. The alloy spectrum shows a small excess of intensity at the edge onset. The loss of charge at the Ag site, anticipated on the basis of the Pd *d*-state filling, would be expected to shift the Ag L_3 absorption edge toward higher energy. On the other hand, if some (albeit small) Ag *d* character states were raised above E_F in the alloy, the *d*-electron–core-hole interaction would shift transitions (at the L_3 edge) to such states to

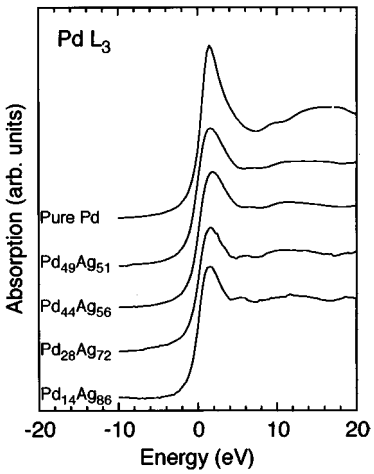

FIG. 5. The Pd L_3 absorption near-edge spectra for a series of ion-beam-mixed Pd-Ag thin films. All data are normalized to unity step height energy well above the edge.

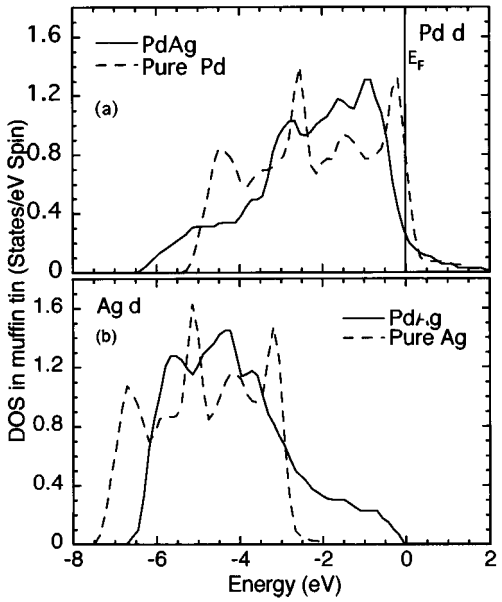

FIG. 6. The *d* density of states in the (a) Ag and (b) Pd spheres for $Pd_{50}Ag_{50}$, with the elemental projected DOS included for comparison, from the calculations of Lu *et al.* (Ref. 35).

lower energy. Thus the weak intensity increases at the Ag L_3 edge onset is at least consistent with some small Ag *d* character near E_F as predicted within the band calculations.[35] It is worth noting that the Ag L_2 edge manifests a similar effect indicating that the proximity of the Pd L_2 edge to the Ag L_3 edge is not the origin of this small effect.

Returning to our Pd L_3 WL results we wish quantitatively to compare the charge transfer in the ion-beam-mixed Pd-Ag alloy to that in the bulk alloys. The $2p \rightarrow 4d$ related white line area, which should reflect directly the *d*-hole count, has been estimated by a method illustrated in Fig. 8. The white line feature rides on top of the continuum step feature, hence this background continuum feature must be subtracted from the L_3 spectra to estimate the white line strength. Since pure Ag has almost no white line feature, we use the pure Ag L_3-edge spectrum to approximate the continuum background.[36] To extract the WL area estimate the pure Ag spectrum is first shifted in energy, so that the inflection point of

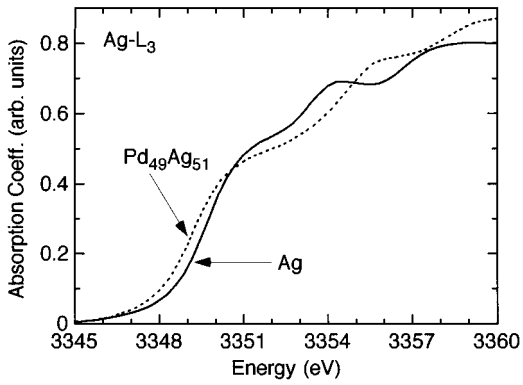

FIG. 7. The near-edge region of the Ag L_3 spectra of the IBM $Pd_{49}Ag_{51}$ alloy and elemental Ag. Note the small excess intensity at the initial edge onset in the IBM alloy.

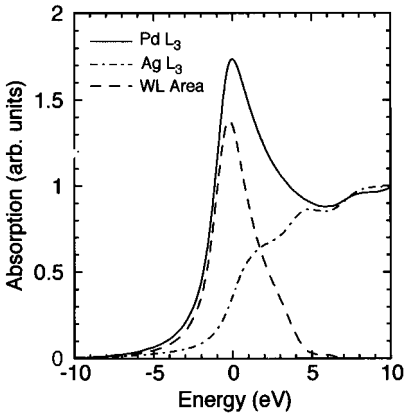

FIG. 8. An example of the method for extracting the white line features. The solid line is the Pd L_3 spectrum of elemental Pd. The dashed-dotted line is the Ag L_3 spectrum. The dashed line is the difference spectrum obtained by subtracting the shifted-Ag spectrum from the elemental Pd spectrum.

the pure Ag spectrum aligns with the WL peak of Pd spectrum in each alloy. The pure Ag spectrum is then subtracted from each Pd L_3 spectrum and resulting area of difference spectrum is used to estimate the number of Pd d holes. The area under the difference spectrum was integrated up to an energy of 4.5 eV above the Pd WL feature peak. This process is similar to Cordts *et al.*'s,[14] and has been used by many other authors in the past to estimate WL area's.[12,13,15,16] As shown in Fig. 9, with increasing Ag concentration, the degree of reduction of the WL area for the ion-beam-mixed alloys is somewhat smaller than that for the bulk alloys. That is, the local density of unoccupied Pd $4d$ states in the ion-beam-mixed alloys is somewhat enhanced relative to that in the bulk alloys. To address the disparity in the Pd d-orbital filling rate, between the bulk and IBM Pd-Ag alloys, we will consider the role of the alloy volume within the macroscopic atomic formalism of de Boer *et al.*[37]

If one formally assembles a compound by bringing dissimilar atoms into contact, there will be discontinuities in the electron density at the boundary of the Wigner-Seitz atomic cells (n_{WS}). Thus the formation of an alloy or a compound requires the equalizing of the n_{WS} of the atoms in contact with each other. Alonso and Girifalco[38] emphasized that this

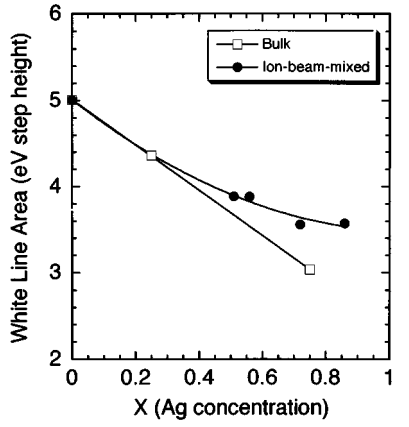

FIG. 9. The areas of the WL features for ion-beam-mixed and bulk Pd-Ag alloys plotted versus alloy concentration.

can be realized by a change in the atomic volume of the two atoms, increasing the volume of the atom with the large electron density and decreasing the volume of the other one until the two densities are equal at the cell boundary. In the case of a transition metal an increase of n_{WS} can be realized by increasing the amount of sp-type charge and decreasing that of d type. That is, the volume of the atomic cell will depend on changes in the d-electron count, due to charge transfer, and on the electron density in the outer region of the atomic cell, n_{WS}.[39,40] According to the macroscopic atomic model of de Boer *et al.*,[37] the approximate relationship between volume and charge transfer upon alloying in a binary system is given by

$$Z_{A \text{ in } A_{1-x}B_x}^{transfer} \simeq \frac{P_Z^*}{a}\left[\frac{(V_A^{2/3})_{alloy}}{(V_A^{2/3})_{pure\ A}} - 1\right], \tag{1}$$

where a is a constant derived from the experimental volume variation in compounds. From experimental volume measurements P_Z^* was found empirically to be about 0.5 electron per (volt·atom) for alloys of two transition metals.[37] In Au-based alloys (for example) the transferred charge estimated thusly, from volume contraction, agrees reasonably well with the number of transferred s electrons, estimated from the corresponding term in the Mössbauer isomer shift.[41]

From Eq. (1), one can easily recognize that the amount of charge transfer depends on the volume change upon alloying, and a larger volume change reflects a larger transfer of d-type charge. Referring to Fig. 1 it should be noted that the average lattice constants of the Ag rich ion-beam-mixed alloys are smaller than those of the bulk alloys. Thus our structural results can be used to estimate the volumes in Eq. (1).

To extract quantitative estimates of the charge transfer indicated by our Pd L_3 studies we will use the recent work of Chen *et al.*[20] in which a linear relation between the $L_{2,3}$ WL area and the $4d$-hole count was found for the latter $4d$ row elements. In this spirit we have used the WL-area difference between Ag and Pd, along with the calculated one electron change in d occupancy between these two elements,[42] to estimate the proportionality constant between the WL area and d-hole count. Using these results, and subtracting the pure Pd hole count, we obtain (from the data in Fig. 9) the estimates of the charge transferred to the Pd d orbitals, as a function of Ag concentration, plotted in Fig. 10. Recall that the volume dependence of the alloy charge transfer, within the macroscopic atom model, was given by Eq. (1). Using this model prediction along with the volume variations from our x-ray data and bulk lattice parameters,[30] we have calculated the relative charge-transfer values expected for these Pd-Ag alloys and plot the results as open squares and circles in Fig. 10, respectively. It can be seen that the agreement between experimental results and the calculated values are satisfactory. Therefore, we suggest that the difference in the local density of unoccupied Pd d state between ion-beam-mixed and bulk Pd-Ag alloys is due to the average atomic volume difference induced by ion-beam mixing.

IV. CONCLUSIONS

We have presented structural results from x-ray diffraction and L_3 edge XAS on ion-beam-mixed, Pd-Ag films, and

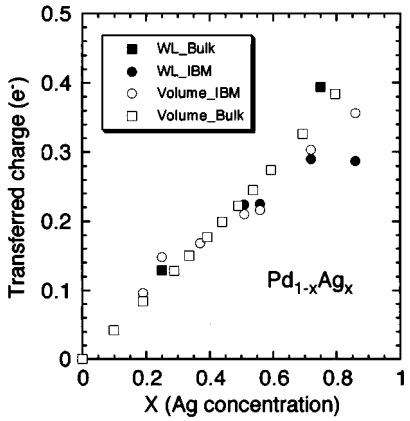

FIG. 10. The number of electrons transferred to Pd, versus the Ag concentration, for ion-beam-mixed (solid squares) and bulk Pd-Ag alloys (filled circles). The charge transfer to Pd, versus Ag concentration, calculated using Eq. (1) for ion-beam-mixed (open squares) and the bulk (open circles) alloys. Here the volumes used were determined from the lattice parameter data shown in Fig. 1.

compared them to selected bulk Pd-Ag alloys. The Ag L_3-edge fine structure features are shifted toward higher energies with increasing Pd content in a manner quantitatively consistent with the Pd-induced lattice compression, as determined from the x-ray diffraction results. These observations support the microscopic alloy formation in these ion-beam-mixed Pd-Ag films.

The density of unoccupied Pd 4*d* states in the ion-beam-mixed Pd-Ag alloys are modified due to the alloy formation. From the arguments of Watson *et al.*[43] based on electronegativity, charge should be transferred to Pd, and this is supported by the WL area decrease at Pd L_3 edge. The similarity of the Ag L_3 x-ray absorption spectra for the ion-beam-mixed, bulk Pd-Ag alloys and pure Ag indicate that the unoccupied partial *d-state* density of Ag is basically unchanged by alloying with Pd. This suggests that the charge transferred away from the Ag is fundamentally *non-d* type as is supported by recent theoretical calculations.[35] The hybridization of some small Ag *d* character into states approaching the Fermi level, as indicated by band structure calculations, is tentatively supported by a small enhancement of intensity at the Ag L_3 edge onset.

The empty density of Pd 4*d* states, for the bulk alloys, is reduced monotonically with increasing Ag concentration, while that for ion-beam-mixed alloys tends to be somewhat larger at high Ag content. This indicates that the degree of charge transfer is larger for bulk Pd-Ag alloys than for the ion-beam-mixed Pd-Ag alloys. The variation of the amount of charge transfer is consistent with the differences of the unit cell volume within the macroscopic atom model.[37]

It is worth reiterating that previous work[14,44] and our work clearly indicate the Pd L_3 WL reduction across the entire Pd-Ag alloy series, and the persistence of appreciable Pd L_3 WL intensity in the dilute Pd end of the alloy series. In our case, for example, at $x=0.5$ the Pd L_3 WL area is reduced by roughly 25%. By roughly integrating the above E_F portions of the calculated Pd *d* DOS in Fig. 5, we obtain an estimate of about 50% reduction between Pd and $Pd_{50}Ag_{50}$.[35] The origin of this excess experimental hole count disparity must at present remain open. A more appropriate definition of the Pd cell in the DOS projection or other improvements in the electronic structure calculations could address this issue. From the XAS point of view transition matrix element enhancement of the Pd *d* states (in the Ag rich materials) or many-body edge singularity corrections at the L_3 edge should be considered.

ACKNOWLEDGMENTS

The present studies were supported in part by the Basic Science Research Institute Program, Ministry of Education, 1994, Project No. BSRI-94-2433 and BSRI-94-2426 and the Korean Science and Engineering Foundation (KOSEF) through the Science Research Center (SRC) of Excellence Program. The travel fund to NSLS was provided by the user program of Pohang Light Source.

[1] B. X. Liu, Phys. Status Solidi A **94**, 11 (1986).
[2] J. C. Plenet, A. Perez, J. Rivory, and O. Laborde, Nucl. Instrum. Methods B **80/81**, 379 (1993).
[3] E. Belin, A. Traverse, and A. Sondor, Nucl. Instrum. Methods B **80/81**, 80 (1993).
[4] F. Lu, N. Stoffel, R. A. Neifeld, S. Gunapala, M. Croft, and M. L. den Boer, Phys. Rev. B **38**, 1508 (1988).
[5] Y. Jeon, N. Jisrawi, G. Liang, F. Lu, M. Croft, W. L. McLean, D. L. Hart, N. G. Stoffel, J. Z. Sun, and T. H. Geballe, Phys. Rev. B **39**, 5748 (1989).
[6] P. A. Lee, P. Citrin, P. Eisenberger, and B. Kincaid, Rev. Mod. Phys. **53**, 769 (1981).
[7] W. T. Elam, J. P. Kirkland, R. A. Neiser, and P. D. Wolf, Phys. Rev. B **38**, 26 (1988).
[8] *EXAFS Spectroscopy, Techniques and Application*, edited by B. K. Teo and D. C. Joy (Plenum Press, New York, 1981).
[9] B. K. Teo, *EXAFS: Basic Principles and Data Anslysis* (Springer-Verlag, Berlin, 1986).
[10] M. Brown, R. Peierls, and E. Stern, Phys. Rev. B **15**, 738 (1977).
[11] L. F. Mattheiss and R. E. Dietz, Phys. Rev. B **22**, 1663 (1980).
[12] F. Lytle, J. Catal. **43**, 376 (1976).
[13] F. Lytle, P. Wei, R. Gregor, G. Via, and J. Sinfelt, J. Chem. Phys. **70**, 4849 (1979).
[14] B. Cordts, D. Pease, and L. V. Azaroff, Phys. Rev. B **24**, 538 (1981).
[15] A. N. Mansour, J. W. Cook, Jr., and D. E. Sayers, J. Phys. Chem. **88**, 2330 (1984).
[16] T. K. Sham, Solid State Commun. **64**, 1103 (1987).
[17] Y. Jeon, Boyun Qi, F. Lu, and M. Croft, Phys. Rev. B **40**, 1538 (1989).
[18] A. Bzowski and T. K. Sham, Phys. Rev. B **48**, 7836 (1993).
[19] A. Bzowski, Y. M. Yiu, and T. K. Sham, Jpn. J. Appl. Phys. **32**, 691 (1993).
[20] J. Chen, M. Croft, Y. Jeon, X. Xu, S. Shaheen, and F. Lu, Phys. Rev. B **46**, 15 639 (1992).
[21] J. Chen, E. Kemly, M. Croft, Y. Jeon, X. Xu, S. A. Shaheen, and

P. H. Ansari, Solid State Commun. **85**, 291 (1993).
[22] C. C. Tyson, A. Bzowski, P. Kristof, M. Kuhn, R. Sammynaiken, and T. K. Sham, Phys. Rev. B **45**, 8811 (1992).
[23] G. M. Stocks, R. W. Williams, and J. S. Faulkner, Phys. Rev. B **4**, 4390 (1971).
[24] J. Eggs and K. Ulmer, Z. Phys. **213**, 293 (1968).
[25] W. Gudat and C. Kunz, Phys. Rev. Lett. **29**, 169 (1972).
[26] Tie Guo and M. L. denBoer, Phys. Rev. B **31**, 6233 (1985).
[27] L. H. Tjeng, C. T. Chen, and S-W. Cheong, Phys. Rev. B **45**, 8205 (1992).
[28] L. G. Parrat, C. F. Hempstead, and E. L. Jossem, Phys. Rev. **105**, 1228 (1957).
[29] S. M. Heald, in *X-ray Absorption; Principles, Applications, Techniques of EXAFS, SEXAFS, and XANES*, edited by D. C. Koningsberger and R. Prins (John Wiley & Sons, New York, 1988), p. 149.
[30] B. R. Coles, J. Inst. Met. **84**, 346 (1956).
[31] Bernd Rauschenbach, Nucl. Instrum. Methods B **80/81**, 303 (1993).
[32] J. J. Rehr and R. C. Albers, Phys. Rev. B **41**, 8139 (1990).
[33] J. J. Rehr, S. I. Zabinsky, and R. C. Albers, Phys. Rev. Lett. **69**, 3397 (1992).
[34] See, B. K. Agrawal, in *X-ray Spectroscopy* (Springer, New York, 1979), Secs. 3.11 and 6.5.
[35] Z. W. Lu, S. H. Wei, and A. Zunger, Phys. Rev. B **44**, 10 470 (1991).
[36] M. Croft, R. Neifeld, and C. U. Segre, Phys. Rev. B **30**, 4164 (1984).
[37] F. R. de Boer, R. Boom, W. C. M. Mattens, A. R. Miedma, and A. K. Niessen, *Cohesion in Metals* (Elsevier Sciences, Amsterdam, 1988).
[38] J. A. Alonso and L. A. Girifalco, J. Phys. F **8**, 2455 (1978).
[39] R. Boom, F. R. de Boer, and A. R. Miedma, J. Less-Common Met. **45**, 237 (1976).
[40] R. Boom, F. R. de Boer, and A. R. Miedma, J. Less-Common Met. **46**, 271 (1976).
[41] A. R. Miedema and F. van der Woude, Physica **100B**, 145 (1980).
[42] G. Materlik, J. E. Muller, and J. W. Wilkins, Phys. Rev. Lett. **50**, 267 (1983).
[43] R. E. Watson, J. W. Davenport, and M. Weinert, Phys. Rev. B **35**, 508 (1987).
[44] M. F. Sorokina and S. A. Nemnonov, Bull. Acad. Sci. USSR, Phys. Ser. **31**, 261 (1967).